Polymer 54 (2013) 3198–3205

Contents lists available at SciVerse ScienceDirect

Polymer

journal homepage: www.elsevier.com/locate/polymer

Synthesis of *N*-[4-Octylphenyl]dithieno[3,2-b:2′,3′-d]pyrrole-based broad absorbing polymers and their photovoltaic applications

Vellaiappillai Tamilavan [a,1], Myungkwan Song [b,1], Sangjun Kim [a], Rajalingam Agneeswari [a], Jae-Wook Kang [c], Myung Ho Hyun [a,*]

[a] *Department of Chemistry, Chemistry Institute for Functional Materials, Pusan National University, Busan 690-735, Republic of Korea*
[b] *Advanced functional Thin films Department, Korea Institute of Materials Science, Changwon, 641-831, Republic of Korea*
[c] *Professional Graduate School of Flexible and Printable Electronics, Department of Flexible and Printable Electronics, Chonbuk National University, Jeonju 561-756, Republic of Korea*

ARTICLE INFO

Article history:
Received 15 February 2013
Received in revised form
17 April 2013
Accepted 20 April 2013
Available online 27 April 2013

Keywords:
Polymer solar cells
Low band gap polymers
Dithieno pyrrole-based polymers

ABSTRACT

Electron rich, fused *N*-aryl pyrrole based monomer namely 2,6-di(4,4,5,5-tetramethyl-1,3,2-dioxaborolan)-*N*-[4-octylphenyl]dithieno[3,2-b:2′,3′-d]pyrrole (*N*-aryl DTP) was synthesized and copolymerized with electron deficient 4,7-bis(5-bromo-3-octyl-2-thienyl)-2,1,3-benzothiadiazole (TBT) to afford alternating polymer **PDTPTBT**. The absorption band of **PDTPTBT** was found to cover the entire visible part of the solar spectrum (300 nm–750 nm) and the optical band gap was estimated to be 1.62 eV. In order to extent the absorption of **PDTPTBT**, another strong electron acceptor unit such as 2,1,3–benzothiadiazole or dimethyl-2H-benzimidazole was incorporated in polymer main chain by copolymerizing three different comonomers (*N*-aryl DTP, TBT and 4,7-dibromo-2,1,3–benzothiadiazole (B) or 4,7-dibromo-2,2-dimethyl-2H-benzimidazole (BI)) at 2:1:1 ratio to afford polymers **PDTPTBTB** and **PDTPTBTBI**, respectively. The absorption band of **PDTPTBTB** and **PDTPTBTBI** was found to be extended up to 1000 nm and 1200 nm, respectively, and the optical band gap was calculated to be 1.33 eV and 1.07 eV, respectively. The HOMO-LUMO energy levels of **PDTPTBT**, **PDTPTBTB** and **PDTPTBTBI** were found to be suitable for polymer solar cell (PSC) applications. The single layer PSCs fabricated with the configuration of ITO/PEDOT:PSS/**PDTPTBT**, **PDTPTBTB** or **PDTPTBTBI**:$PC_{60}BM$(1:3 wt/wt)/LiF/Al showed maximum power conversion efficiency (*PCE*) of 2.04%, 1.01% and 0.70%, respectively.

1. Introduction

Polymer based bulk heterojunction solar cells (PSCs) have attracted much attention due to their advantages in that they are green energy production techniques and the light weight-flexible PSC devices can be easily fabricated to large area at low cost by standard roll-to-roll printing techniques [1,2]. The solar to electrical energy conversion efficiency (*PCE*) of the PSCs has been improved up to 7–9.2% [3,4,5,6,7] for single PSCs and 8–10.6% [8,9,10] for tandem structured PSCs containing two photoactive layers made up with two different donor polymers that can absorb the sunlight at different interval of the solar spectrum. The theoretical studies implied that the maximum *PCE* could reach up to 17% for single layer PSCs and 24% for tandem PSCs [11]. Presently, several attempts such as developing structurally new donor polymers having the appropriate energy levels with effective light harvesting ability [3,4,5,6,7], replacing the existing electron accepting $PC_{60}BM$ or $PC_{71}BM$ derivatives with new acceptor materials having higher LUMO energy level [12] and fine tuning the PSC device structure to inverted or tandem architectures [8,9,10] are in progress with the aim of enhancing the PSC device performances. In our attempt to improve the *PCE* of PSCs, we were interested in preparing new broad absorbing polymers because the *PCE* of PSCs strongly depends on the light harvesting ability of the donor polymers. So far, the broad absorption polymers have been prepared by copolymerizing the electron rich and electron deficient unit in alternate fashion and thereby the band gap of the polymers decreased due to the combined electronic transitions such as $\pi-\pi^*$ and internal charge transfer (ICT) between the donor and acceptor moiety [13,14,15,16,17,18,19,20].

Recently, we prepared thiophene-(*N*-aryl)pyrrole-thiophene (*N*-aryl TPT) based electron rich monomers and copolymerized them with various electron rich and electron deficient comonomers with the aim of preparing *N*-aryl TPT based polymers showing dissimilar absorption and energy levels for PSC applications [21,22,23,24,25,26,27,28]. The photovoltaic studies on *N*-aryl TPT

---

[*] Corresponding author. Tel.: +82 51 510 2245; fax: +82 51 516 7421.
E-mail address: mhhyun@pusan.ac.kr (M.H. Hyun).
[1] These authors made equal contribution to this work.

0032-3861/$ – see front matter © 2013 Elsevier Ltd. All rights reserved.
http://dx.doi.org/10.1016/j.polymer.2013.04.049

based homo polymer (**PTPT**) [21] and copolymers containing phenylene (**PPTPT**) [21], thiophene (**PTTPT**) [21], indenofluorene (**PIFTPT**) [22], thiadiazoloquinoxaline (**TPyTDzQ**) [23], 2,1,3–benzothiadiazole (**TPyTBz**) [24,25] or thiophene–2,1,3–benzothiadiazole–thiophene (**PTPTTBT** and **PTTPTTB**) [26,27] were found to show maximum *PCE* of 2.03% with an open-circuit voltage (V_{oc}) of 0.57 V, a short-circuit current density (J_{sc}) of 9.27 mA/cm^2, and a fill factor (*FF*) of 38.4% for **PTTPTTB**–based PSC device [27]. The absorption bands of the polymers **PTPTTBT** and **PTTPTTB** were found to be quite broad and flat from 300 nm to 700 nm [26,27]. The broad and flat absorption of polymers **PTPTTBT** and **PTTPTTB** induced us to develop fused thiophene–(*N*-aryl)pyrrole–thiophene (*N*-aryl-dithiophenepyrrole, *N*-aryl DTP) based monomer unit because *N*-aryl DTP unit is expected to show better π–π conjugation and planarity compared with those of *N*-aryl TPT units. Recently several electron donor polymers containing fused electron rich units have been reported to show broad absorption and high carrier mobility [29]. *N*-Aryl DTP based polymers are also expected to show relatively red shifted absorption and better carrier mobility.

In this study, we prepared a new alternating copolymer, **PDTPTBT**, by copolymerizing the newly synthesized *N*-aryl DTP monomer with 4,7-bis(5-bromo-3-octyl-2-thienyl)-2,1,3-benzothiadiazole (TBT) monomer and we also incorporated 2,1,3–benzothiadiazole or 2,2-dimethyl-2H-benzimidazole unit in the **PDTPTBT** main chain to afford polymer **PDTPTBTB** or polymer **PDTPTBTBI**, respectively, with the aim of extending the absorption range. Here, we wish to report the detailed synthesis, opto-electrical and photovoltaic properties of three new *N*-aryl DTP–based polymers including **PDTPTBT**, **PDTPTBTB** and **PDTPTBTBI**.

2. Experimental section

2.1. Materials and instruments

The commercially available reagents were received from Aldrich or TCI chemicals and used without further purification. The common organic solvents such as dichloromethane, tetrahydrofuran and diethyl ether were distilled and handled in a moisture-free atmosphere. The purification of the newly synthesized compounds was performed by column chromatography on silica gel (Merck Kieselgel 60, 70–230 mesh ASTM). The ^{1}H and ^{13}C NMR spectra of the compounds were recorded using Varian Mercury Plus spectrometer (300 MHz and 75 MHz, respectively) in $CDCl_3$. Gel permeation chromatography (GPC) analyses were conducted on an Agilent 1200 Infinity Series separation module using polystyrene as a standard and chloroform as an eluent to determine the molecular weight and polydispersity (PDI) of the polymers. Thermogravimetric analyses (TGA) were conducted with a TA instrument Q500 at a heating rate of 10 °C/min under nitrogen. The photophysical studies of the polymers were performed on JASCO V-570 spectrophotometer at 25 °C in chloroform or as thin films on glass. Cyclic voltammetry (CV) measurements were performed using a CH Instruments Electrochemical Analyzer with Ag/AgCl reference electrode, platinum as a working and counter electrode in a 0.1 M tetrabutylammonium tetrafluoroborate (Bu_4NBF_4) as the supporting electrolyte at room temperature. Atomic force microscopy (AFM) images of blend films were obtained on a Veeco-Multimode AFM operating in the tapping mode.

2.2. Device fabrication and characterization of BHJ solar cells

The polymer solar cells were constructed as follows. The transparent ITO electrode (80 nm thick, 20 Ω/sq sheet resistance) was coated on glass substrates and cleaned by ultrasonication sequentially in detergent, deionized water, acetone, and isopropyl alcohol. After drying the substrates, a 40 nm thick layer of poly(3,4-ethylenedioxythiophene):poly(styrenesulfonate) (PEDOT:PSS) (CLEVIOUS, P) was spin-coated (1000/5000 rpm, 30 s) onto the precleaned and UV-ozone treated ITO substrates and baked in air at 120 °C for 10 min. Subsequently, the 80 nm thickness of active layer (polymer:$PC_{60}BM$ blend solution) was spin coated (300/600 rpm, 40 s) onto the ITO/PEDOT:PSS substrates. The polymer:$PC_{60}BM$ blend solution was prepared by mixing each of the polymers and $PC_{60}BM$ solution in a weight ratio of 1:1, 1:2 or 1:3 in 1,2-dichlorobenzene. After drying the solvent, 0.7 nm thick layer of LiF was deposited on the substrates. Subsequently, 120 nm thick layer of Al was deposited through a shadow mask on top of the ITO/PEDOT:PSS/polymer:$PC_{60}BM$/LiF substrates under high vacuum (1.2×10^{-6} torr). The top metal electrode area, comprising the active area of the solar cells, was found to be 0.36 cm^2. The BHJ solar cell performance was measured using a AM 1.5G solar simulator (Oriel 300 W) at 100 mW/cm^2 light illumination after adjusting the light intensity using Oriel power meter (model No. 70260 which was calibrated using laboratory standards that are traceable to the National Institute of Standards and Technologies, USA). Current-voltage (*J*–*V*) characteristics of the polymer BHJ solar cell devices were measured using a standard source measurement unit (Keithley 236). All fabrication steps and characterization measurements were performed in an ambient environment without a protective atmosphere. The thickness of the thin films was measured using a KLA Tencor Alpha-step IQ surface profilometer with an accuracy of ±1 nm.

2.3. Synthesis of polymers

2.3.1. Synthesis of N-[4-octylphenyl]dithieno[3,2-b:2′,3′-d]pyrrole (*1*)

A stirred solution of 3,3′-dibromo-2,2′-bithiophene (5.2 g, 16 mmol), which was prepared via the known procedure [30], in 40 mL of toluene was purged well with argon for 15 min, and then NaO*t*Bu (3.7 g, 38.5 mmol), Pd_2dba_3 (0.4 g, 0.44 mmol), and 1,1′-bis(diphenylphosphine)ferrocene (DPPF, 1.0 g, 1.8 mmol) were added in sequence. Then, 4-octylaniline (4.0 mL, 18 mmol) was added, and the mixture was refluxed for 12 h. The mixture was allowed to cool down, and the solvent was removed by rotary evaporation. The solid residue was dissolved in dichloromethane and the insoluble precipitates were filtered off. The organic solution was washed with water and then brine, and dried over anhydrous Na_2SO_4. The solvent was removed by rotary evaporation and the crude product was purified by column chromatography (silica gel, hexane:CH_2Cl_2, 90/10) to afford compound **1** as a white solid. Yield: 5.4 g (92%). mp 79–80 °C; ^{1}H NMR (300 MHz, $CDCl_3$): δ (ppm) 7.49 (d, 2H), 7.33 (d, 2 H), 7.17 (s, 4 H), 2.68 (t, 2 H), 1.60–1.74 (m, 2 H), 1.22–1.44 (m, 10 H), 0.90 (t, 3 H); ^{13}C NMR (75 MHz, $CDCl_3$): δ (ppm) 144.4, 141.2, 137.8, 129.9, 123.5, 122.8, 116.8, 112.5, 35.8, 32.1, 31.7, 29.7, 29.6, 29.5, 22.9, 14.4; HRMS (EI$^+$, *m*/*z*) [M$^+$] Calcd for $C_{22}H_{25}NS_2$ 367.1428, found 367.1434.

2.3.2. Synthesis of 2,6-dibromo-N-[4-octylphenyl]dithieno[3,2-b:2′,3′-d]pyrrole (*2*)

Compound **1** (4.0 g, 10.8 mmol) was dissolved in chloroform (30 mL) and cooled to 0 °C in ice bath under argon. *N*-Bromosuccinimide (NBS) (4.25 g, 23.9 mmol) was added in one portion to the stirred solution. After 15 min, the mixture was allowed to warm to room temperature and stirred for 5 h. The organic mixture was washed with water and then brine and dried over anhydrous Na_2SO_4. The solution was filtered and evaporated by rotary evaporation and the crude product was purified by column chromatography (silica gel, hexane:CH_2Cl_2, 90/10) to afford pure compound **2** as a yellowish solid. Yield: 5.4 g (92%). mp 121–122 °C;

^{1}H NMR (300 MHz, $CDCl_3$): δ (ppm) 7.49 (d, 2H), 7.32 (d, 2 H), 7.16 (s, 2 H), 2.67 (t, 2H), 1.60–1.74 (m, 2 H), 1.22–1.44 (m, 10 H), 0.89 (t, 3H); ^{13}C NMR (75 MHz, $CDCl_3$): δ (ppm) 142.1, 141.1, 136.8, 130.0, 123.0, 116.6, 115.7, 110.5, 35.7, 32.1, 31.7, 29.7, 29.6, 29.5, 22.9, 14.4; HRMS (EI$^+$, *m*/*z*) [M$^+$] Calcd for $C_{22}H_{23}Br_2NS_2$ 522.9639, found 522.9647.

2.3.3. Synthesis of 2,6-di(4,4,5,5-tetramethyl-1,3,2-dioxaborolan)-N-[4-octylphenyl]dithieno[3,2-b:2′,3′-d]pyrrole (N-aryl DTP)

Under argon atmosphere, a solution of compound **2** (1.84 g, 3.50 mmol) in dry THF (40 mL) was cooled to −78 °C in a dry ice-acetone bath for 20 min. To the stirred solution, n-BuLi (3.10 mL, 7.7 mmol, 2.5 M solution in hexane) was added dropwise and stirred for 20 min in the same bath. Then, the mixture was allowed to warm to room temperature and stirred for 45 min. The solution was again cooled to −78 °C for 20 min and then 2-isopropoxy-4,4,5,5-tetramethyl-1,3,2-dioxaborolane (1.65 mL, 8.00 mmol) was added dropwise. The solution was slowly warmed to room temperature and stirred for overnight. The organic mixture was washed with water and then brine, and dried over anhydrous Na_2SO_4. The solvents were filtered and removed by rotary evaporation and the crude product was purified by column chromatography (silica gel, hexane:ethyl acetate, 90/10) to afford pure product, *N*-aryl DTP, as a light yellow color solid. Yield: 1.01 g (47%). mp 260–261 °C; ^{1}H NMR (300 MHz, $CDCl_3$): δ (ppm) 7.66 (s, 2 H), 7.49 (d, 2 H), 7.28 (d, 2 H), 2.66 (t, 2 H), 1.58–1.72 (m, 2 H), 1.20–1.40 (m, 34 H), 0.90 (t, 3 H); ^{13}C NMR (75 MHz, $CDCl_3$): δ (ppm) 147.8, 141.3, 137.4, 129.8, 123.1, 121.3, 84.4, 35.7, 32.1, 31.7, 29.7, 29.6, 29.5, 25.0, 22.9, 14.4; HRMS (EI$^+$, *m*/*z*) [M$^+$] Calcd for $C_{34}H_{47}B_2NO_4S_2$ 619.3133, found 619.3139.

2.3.4. Synthesis of 4,7-dibromo-2,2-dimethyl-2H-benzimidazole (BI)

4,7-Dibromo-2,2-dimethyl-2H-benzimidazole was synthesized using the similar reported procedures for the preparation of 2,2-dimethyl-2H-benzimidazole [31,32]. Here, we used 3,6-dibromobenzene-1,2-diamine as a starting material instead of benzene-1,2-diamine. A stirred solution of 3,6-dibromobenzene-1,2-diamine (7.9 g, 30 mmol), which was prepared via the known procedure [33], in 160 mL of ethyl acetate was added a solution of copper(II) perchlorate hexahydrate ($Cu(II)(ClO_4)_2.6H_2O$ (22.2 g, 60 mmol) in 90 mL anhydrous ethanol at room temperature. The mixture was stirred for 30 min and the solid material was filtered and washed with 100 mL of ethyl acetate:ethanol (8:2) mixture. The solid material was dried under vacuum to afford pure product of bis(3,6-dibromobenzene-1,2-diamine)copper(II) perchlorate (**3**) as a gray color solid. Yield: 10.5 g (60%). mp 290–291 °C; ^{1}H NMR (300 MHz, DMSO-d^6): δ (ppm) 6.60 (s, 2 H), 4.93(brd s, 8 H). Compound **3** (8.0 g, 13.5 mmol) and 480 mL of purified acetone were stirred at room temperature under argon atmosphere. After 6 h, the precipitates were filtered off from the solution and washed with 200 mL acetone. The solid materials were dried under vacuum to afford pure product of 4,7-dibromo-2,2-dimethyl-2H-benzimidazole copper(I) perchlorate (**4**) as a dark brown solid. Yield: 3.3 g (52%). mp 239–240 °C; ^{1}H NMR (300 MHz, DMSO-d^6): δ (ppm) 7.45 (s, 2 H), 1.48 (s, 6 H). Compound **4** (2.5 g, 5.35 mmol) in 200 mL of chloroform was added 100 mL of 28–30% aqueous ammonia solution. The resulting solution was stirred at room temperature for 1 h. Then, the mixture was poured into water and the organic layer was separated. The aqueous layer was extracted one more time with chloroform and the combined organic layer was washed with water and then brine, and dried over anhydrous Na_2SO_4. The solvent was removed by rotary evaporation and the crude product was purified by column chromatography (silica gel, hexane:ethyl acetate, 90/10) to afford compound **BI** as a yellow solid. Yield: 1.3 g (80%). The characterization data was found to be identical with the reported data [34].

2.3.5. General procedure for polymer synthesis

A solution of respective monomers (shown in Scheme 2) in toluene (40 mL) was purged well with argon for 45 min. Then, $Pd(PPh_3)_4$ (0.02 g, 5 mol %) and 2 M K_2CO_3 solution were added to the stirred solution and the mixture was heated to reflux under argon atmosphere. After refluxing for 48 h, 50 mg of phenylboronic acid was added. The whole mixture was refluxed for 6 h and then 0.1 mL of bromobenzene was added and refluxed again for 6 h.

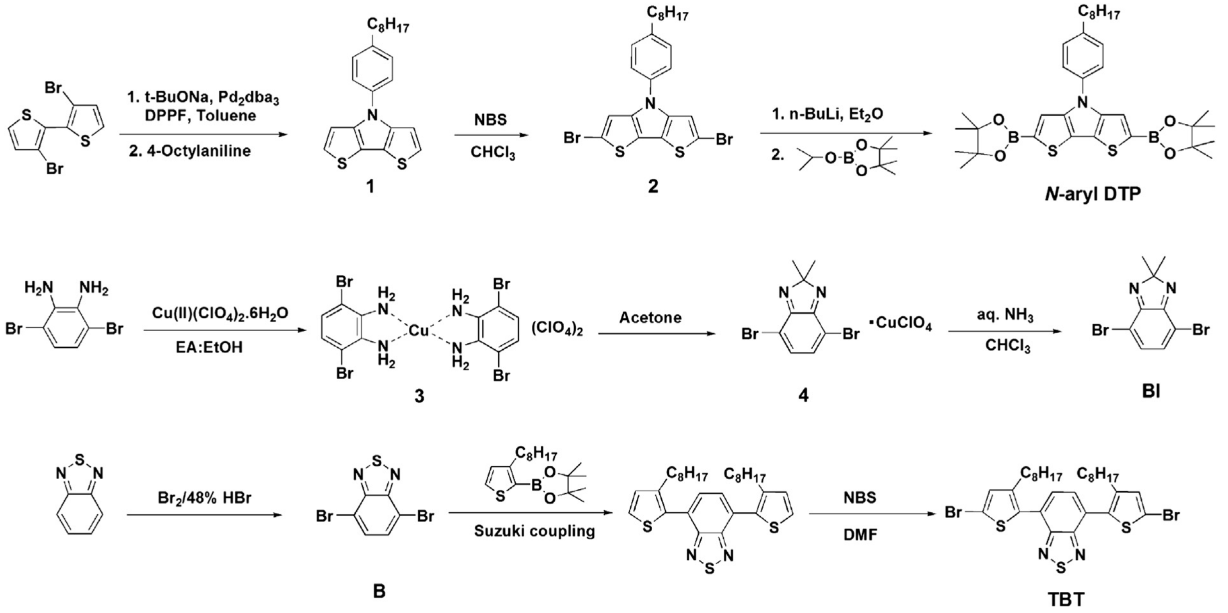

Scheme 1. Synthetic route for the synthesis of *N*-aryl DTP, BI and TBT.

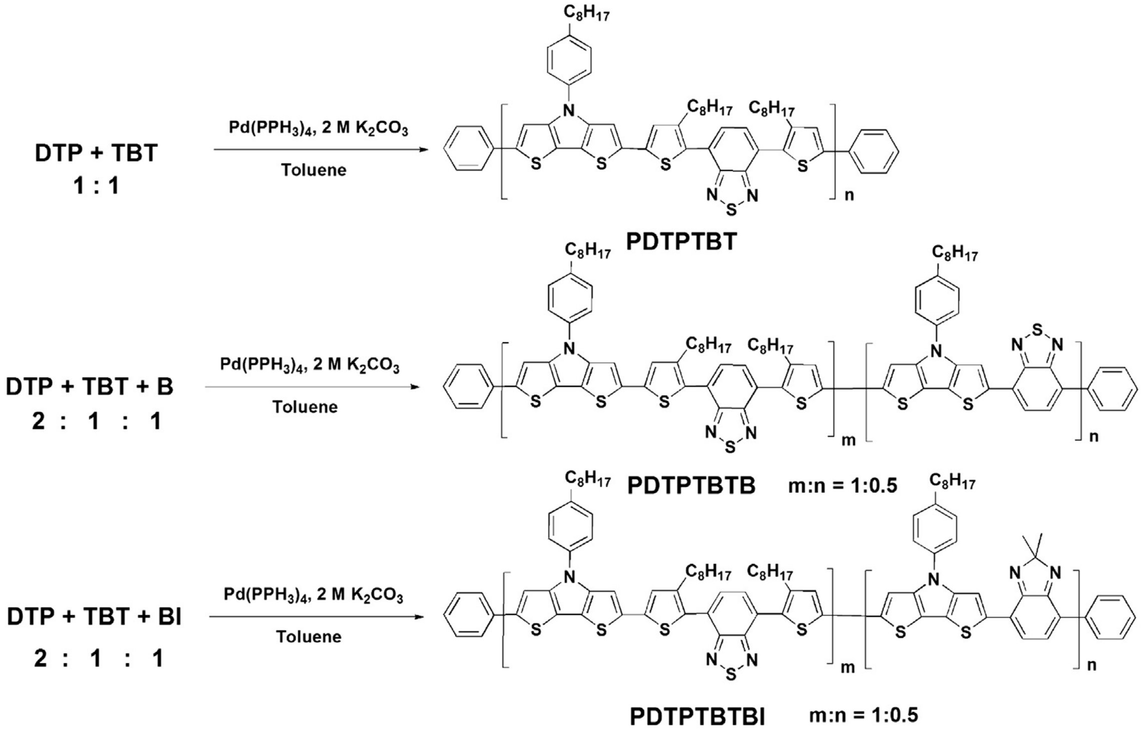

Scheme 2. Synthetic route for the synthesis of **PDTPTBT**, **PDTPTBTB** and **PDTPTBTBI**.

Then, the reaction mixture was cooled to room temperature and then poured into the mixed solvent of methanol and water (100 mL:50 mL) with vigorous stirring. The precipitate was recovered by filtration, and then extracted with methanol for 24 h and acetone for 24 h in a Soxhlet apparatus. **PDTPTBT**: Black color, Yield (0.30 g, 78%). ^{1}H NMR (300 MHz, CDCl3): δ 7.58–7.72 (m, 2 H), 7.44–7.54 (m, 2 H), 7.38 (d, 2 H), 7.26–7.30 (m, 2 H), 7.16–7.26 (m, 2 H), 2.50–2.80 (m, 6 H), 1.50–1.80 (m, 6 H), 1.00–1.50 (m, 30 H), 0.70–1.00 (m, 9 H). **PDTPTBTB**: Black color, Yield (0.26 g, 46%). ^{1}H NMR (300 MHz, CDCl3): δ 7.58–7.72 (m, 3 H), 7.46–7.56 (m, 3 H), 7.26–7.42 (m, 6 H), 7.16–7.26 (m, 2 H), 2.50–2.80 (m, 7 H), 1.60–1.80 (m, 4 H), 1.50–1.60 (m, 3 H), 1.00–1.50 (m, 35 H), 0.70–1.00 (m, 11 H). **PDTPTBTBI**: Black color, Yield (0.30 g, 46%). ^{1}H NMR (300 MHz, CDCl3): δ 7.58–7.72 (m, 3 H), 7.46–7.56 (m, 3 H), 7.26–7.42 (m, 6 H), 7.16–7.26 (m, 2 H), 2.50–2.80 (m, 7 H), 1.60–1.80 (m, 7 H), 1.50–1.60 (m, 3 H), 1.00–1.50 (m, 35 H), 0.70–1.00 (m, 11 H).

3. Results and discussions

3.1. Synthesis and characterization of polymers

The synthetic procedures for the monomers such as *N*-aryl DTP and BI and polymers **PDTPTBT**, **PDTPTBTB** and **PDTPTBTBI** are outlined in Scheme 1 and Scheme 2, respectively. The electron deficient comonomers such as B and TBT were synthesized by using the reported procedure [26] as shown in Scheme 1. The electron rich new *N*-aryl DTP monomer namely 2,6-di(4,4,5,5-tetramethyl-1,3,2-dioxaborolan)-N-[4-octylphenyl]dithieno[3,2-b:2′,3′-d]pyrrole was synthesized from the similar procedure reported by Koeckelberghs et al. [30]. The reaction between 3,3′-dibromo-2,2′-bithiophene and 4-octylaniline in the presence of palladium catalyst afforded compound **1**. Compound **1** was then brominated by using NBS to afford compound **2**. The final *N*-aryl DTP monomer was obtained by treating compound **2** with n-BuLi followed by 2-isopropoxy-4,4,5,5-tetramethyl-1,3,2-dioxaborolane. Electron deficient 4,7-dibromo-2,2-dimethyl-2H-benzimidazole (BI) was synthesized via the method similar to the reported procedures for the preparation of 2,2-dimethyl-2H-benzimidazole [31,32,33]. To the stirred solution of 3,6-dibromobenzene-1,2-diamine in ethyl acetate was added a solution of copper(II) perchlorate hexahydrate in anhydrous ethanol to afford compound **3**. Compound **3** was stirred with acetone to afford compound **4**. The copper(I) perchlorate in compound **4** was removed by treating with aqueous ammonia solution to afford BI in good yield. The method used in this study for the preparation of BI is expected to be more facile than the method reported recently [34]. The Suzuki polycondensation of the two monomers such as *N*-aryl DTP and TBT afforded alternating polymer **PDTPTBT**. The Suzuki random copolymerization of the monomers including *N*-aryl DTP, TBT and B at 2:1:1 ratio or including DTP, TBT and BI at 2:1:1 ratio yielded polymers **PDTPTBTB** and **PDTPTBTBI**, respectively. The

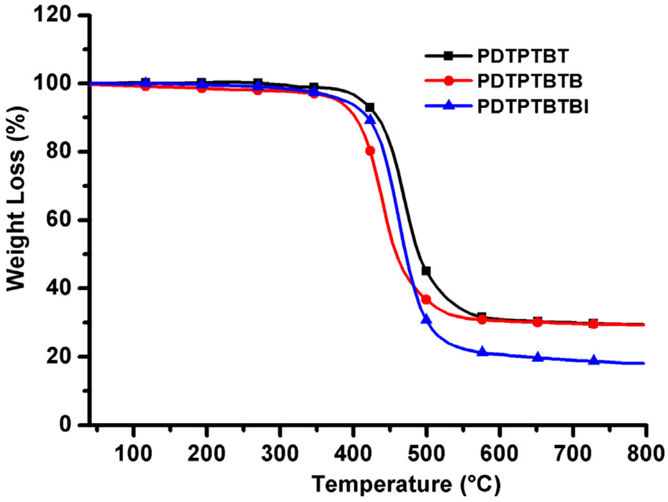

Fig. 1. TGA curves of **PDTPTBT**, **PDTPTBTB** and **PDTPTBTBI**.

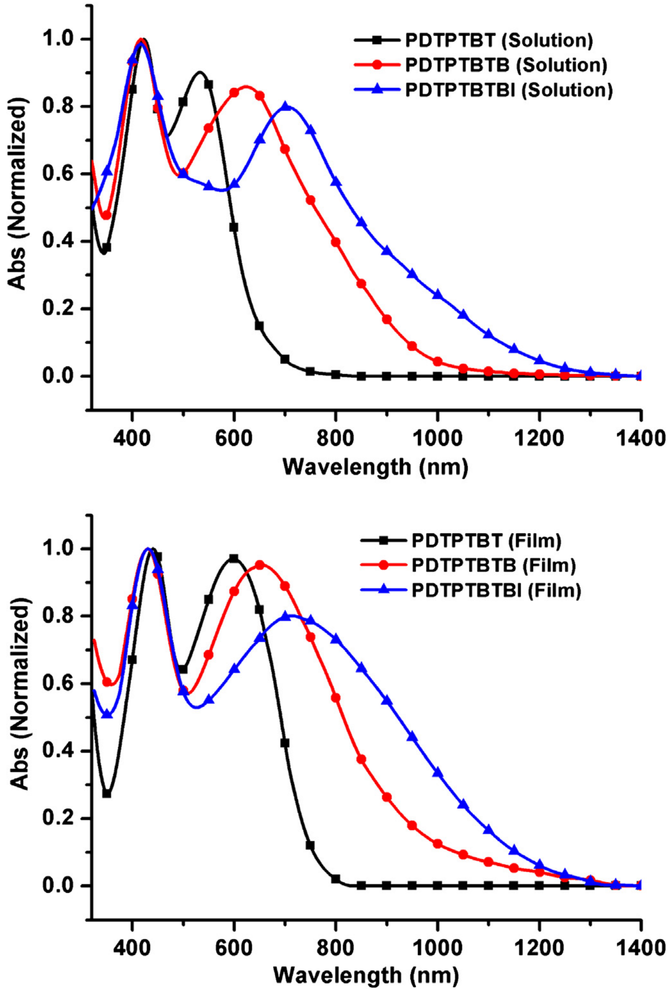

Fig. 2. UV–visible–NIR absorption spectra of **PDTPTBT**, **PDTPTBTB** and **PDTPTBTBI** in chloroform and thin film on glass.

careful ^{1}H NMR analysis of the polymers **PDTPTBTB** and **PDTPTBTBI** revealed the presence of all three monomers such as *N*-aryl DTP, TBT and B or BI in their main chain at different ratios. The two different repeating unit [TBT based repeating unit (m) and 2,1,3-benzothiadiazole or 2,2-dimethyl-2H-benzimidazole based repeating unit (n)] ratios of both polymers, **PDTPTBTB** and **PDTPTBTBI**, were determined to be 1:0.5. The solubility of the polymers was tested in the common organic solvents such as chloroform, tetrahydrofuran, chlorobenzene and dichlorobenzene. The solubility of **PDTPTBT** was found to be excellent in all common organic solvents mentioned above, whereas polymers **PDTPTBTB** and **PDTPTBTBI** showed good solubility in chlorobenzene and dichlorobenzene, but relatively poor solubility in chloroform and tetrahydrofuran at room temperature. The GPC analysis revealed that the weight average molecular weights (M_w) of polymers **PDTPTBT**, **PDTPTBTB** and **PDTPTBTBI** were 2.21×10^4, 9.06×10^3 and 1.40×10^4 and their polydispersities were 1.95, 1.45, and 1.82, respectively. The thermal stability of the polymers **PDTPTBT**, **PDTPTBTB** and **PDTPTBTBI** was determined by using thermogravimetric analysis (TGA), and the 5% decomposition temperature was found to be 407 °C, 377 °C and 376 °C, respectively. Fig. 1 displays the TGA curve of polymers **PDTPTBT**, **PDTPTBTB** and **PDTPTBTBI**.

3.2. Optical properties

The UV-visible-NIR absorption spectra of **PDTPTBT**, **PDTPTBTB** and **PDTPTBTBI** in a chloroform solution and as thin film on glass are shown in Fig. 2. All absorption spectra of **PDTPTBT**, **PDTPTBTB** and **PDTPTBTBI** showed their first absorption maxima almost at the same wavelength, but the second absorption maxima were found to be significantly red shifted in the order of **PDTPTBT** < **PDTPTBTB** < **PDTPTBTBI**. The absorption maxima (λ_{max}) of **PDTPTBT** were observed at 423 nm and 533 nm in chloroform and at 441 nm and 597 nm as thin film while those of random polymer **PDTPTBTB** were observed at 417 nm and 624 nm in chloroform and at 430 nm and 653 nm as thin film and those of **PDTPTBTBI** were observed at 423 nm and 703 nm in chloroform and 431 nm and 716 nm as thin film. The film state absorption bands of **PDTPTBT**, **PDTPTBTB** and **PDTPTBTBI** were found to be slightly broader than the solution state bands and their corresponding absorption maxima were red shifted compared to those observed in solution state. The later phenomenon indicates that the polymers are well oriented (better π–π interchain interaction) in film state than those in solution state. In our previous study, we demonstrated that polymer **PTPTTBT** incorporating both of *N*-aryl TPT and TBT units shows a broad and flat absorption maximum resulting from the overlap of the two π–π^* electronic transitions originated from the *N*-aryl TPT and TBT units [26,27]. Similarly, the absorption spectrum of **PDTPTBT** is expected to be resulted from the overlap of the two π–π^* electronic transitions originated from the *N*-aryl DTP and TBT units. On the other hand, the absorption bands of **PDTPTBTB** and **PDTPTBTBI** are expected to be attributed to the combination of the π–π^* electronic transitions and the donor–acceptor internal charge transfer (ICT) between *N*-aryl DTP and 2,1,3–benzothiadiazole or dimethyl-2H-benzimidazole. The electron attracting ability of the electron deficient units used in this study is expected in the following order of TBT < B < BI, and, consequently, the absorption bands of the polymers were found to be red shifted in the order of **PDTPTBT** < **PDTPTBTB** < **PDTPTBTBI**. The optical band gaps of **PDTPTBT**, **PDTPTBTB** and **PDTPTBTBI** were calculated from the onset wavelength of the optical absorption in thin film to be 1.62 eV, 1.33 eV, and 1.07 eV, respectively. As

Table 1
Polymerization results, thermal, optical and electrochemical properties of polymers PDTPTBT, PDTPTBTB and PDTPTBTBI.

	M_w[a]	PDI[a]	TGA[b] (°C)	λ_{max} in solution (nm)[c]	λ_{max} as film (nm)[d]	$E_{g,\ opt}$ (eV)[e]	HOMO (eV)[f]	LUMO (eV)[f]	$E_{g,\ elc}$ (eV)[g]
PDTPTBT	2.21×10^4	1.95	407	423, 533	441, 597	1.62	−5.27	−3.57	1.70
PDTPTBTB	9.06×10^3	1.45	377	417, 624	430, 653	1.33	−5.01	−3.66	1.35
PDTPTBTBI	1.40×10^4	1.82	376	423, 703	431, 716	1.07	−4.94	−3.76	1.18

[a] Weight average molecular weight (M_w) and polydispersity (PDI) of the polymers were determined by GPC using polystyrene standards.
[b] 5% weight loss temperature measured by TGA under N_2.
[c] Measurements were performed in chloroform solution.
[d] Measurements in thin film were performed on glass.
[e] Band gap estimated from the onset wavelength of the optical absorption in thin film.
[f] The HOMO and LUMO levels of the polymers were estimated from cyclic voltammetry analysis.
[g] Band gap estimated from the HOMO and LUMO levels estimated from the cyclic voltammetry analysis.

our expectation, polymer **PDTPTBT** showed significantly broader absorption band than the reported polymer PTPTTBT and the optical band gap of **PDTPTBT** was found to be 0.32 eV lower than that of PTPTTBT [26]. The optical properties of **PDTPTBT**, **PDTPTBTB** and **PDTPTBTBI** are summarized in Table 1.

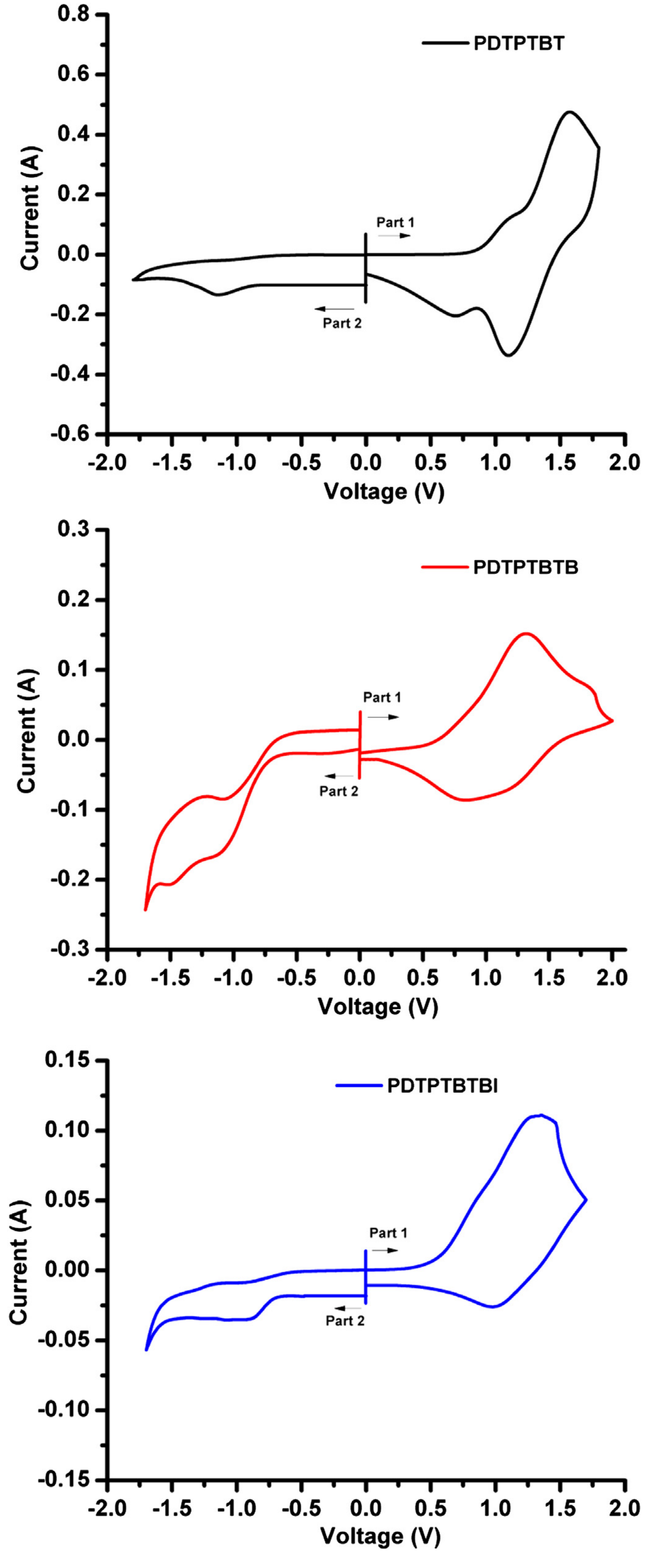

Fig. 3. Cyclic voltammograms of **PDTPTBT**, **PDTPTBTB** and **PDTPTBTBI** as films on platinum working electrode in 0.1 M Bu_4NBF_4/acetonitrile at 100 mV/s, potential vs. Ag/AgCl.

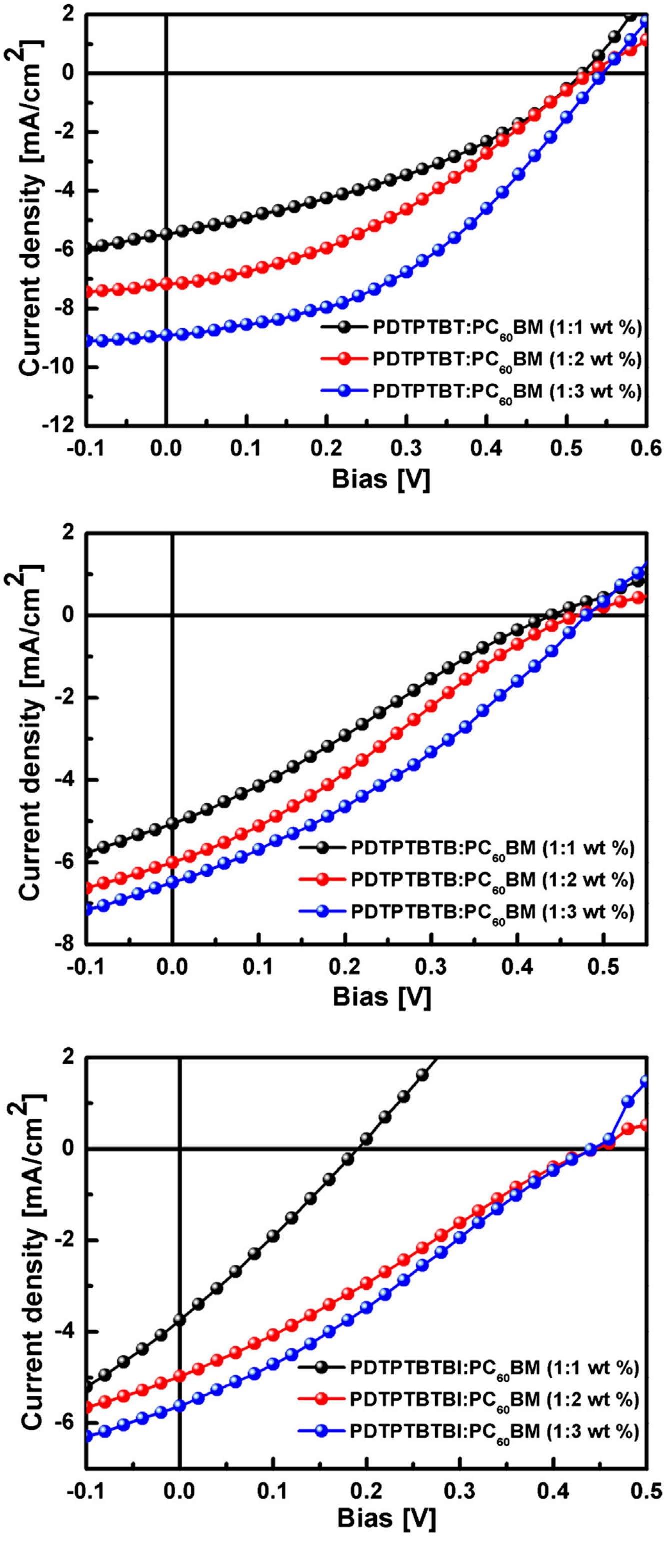

Fig. 4. *J-V* characteristics of PSCs prepared from ITO/PEDOT:PSS/**PDTPTBT** or **PDTPTBTB** or **PDTPTBTBI**:$PC_{60}BM$/LiF/Al under AM 1.5 irradiation (100 mW/cm^2).

Table 2
Solar cell performance of PDTPTBT, PDTPTBTB and PDTPTBTBI as electron donors with $PC_{60}BM$ as an electron Acceptor in ITO/PEDOT:PSS/Polymer:$PC_{60}BM$/LiF/Al device.

Photoactive active layer	J_{sc} (mA/cm^2)[a]	V_{oc} (V)[b]	FF (%)[c]	PCE (%)[d]
PDTPTBT : $PC_{60}BM$ (1:1 wt/wt)	5.47	0.52	36.67	1.04
PDTPTBT : $PC_{60}BM$ (1:2 wt/wt)	7.16	0.53	36.57	1.38
PDTPTBT : $PC_{60}BM$ (1:3 wt/wt)	**8.91**	**0.55**	**42.09**	**2.04**
PDTPTBTB : $PC_{60}BM$ (1:1 wt/wt)	5.06	0.44	26.30	0.58
PDTPTBTB : $PC_{60}BM$ (1:2 wt/wt)	6.00	0.47	27.46	0.77
PDTPTBTB : $PC_{60}BM$ (1:3 wt/wt)	**6.48**	**0.48**	**32.73**	**1.01**
PDTPTBTBI : $PC_{60}BM$ (1:1 wt/wt)	3.74	0.19	26.80	0.19
PDTPTBTBI : $PC_{60}BM$ (1:2 wt/wt)	4.97	0.44	26.80	0.59
PDTPTBTBI : $PC_{60}BM$ (1:3 wt/wt)	**5.62**	**0.44**	**28.20**	**0.70**

[a] Short-circuit current density.
[b] Open-circuit voltage.
[c] Fill factor.
[d] Power conversion efficiency.

3.3. Electrochemical properties

Determination of the highest occupied molecular orbital (HOMO) and lowest unoccupied molecular orbital (LUMO) energy levels of the synthesized polymers is essential to evaluate their suitability for BHJ solar cell applications. For the efficient charge separation at the donor (polymer)–acceptor ($PC_{60}BM$) interface, the LUMO level of the polymer should be above the LUMO level of $PC_{60}BM$ by at least 0.2–0.3 eV [35]. In addition, to achieve higher voltage (V_{oc}) in BHJ solar cells, the deeper HOMO energy level of the electron donor material is preferable since the theoretical V_{oc} is defined as the energy difference between the HOMO level of the polymer and LUMO level of the acceptor [35]. The HOMO and LUMO energy levels of the polymers were estimated from the cyclic voltammetry (CV) analysis. Fig. 3 represents the cyclic voltamograms of **PDTPTBT**, **PDTPTBTB** and **PDTPTBTBI**. All three polymers were showed reversible electrochemical behaviors. The HOMO and LUMO energy levels of the polymers were calculated from their onset oxidation ($E_{ox,\ onset}$) and reduction ($E_{red,\ onset}$) potential values by using the following equations, $E_{HOMO} = -(E_{ox,\ onset} + 4.4)$ eV and $E_{LUMO} = -(E_{red,\ onset} + 4.4)$ eV [23,36]. The $E_{ox,\ onset}$ and $E_{red,\ onset}$ potentials of **PDTPTBT**, **PDTPTBTB** and **PDTPTBTBI** were determined by the carful CV analysis to be 0.87 V, 0.61 V, 0.54 V and −0.83 V, −0.74 V, −0.64 V, respectively. The HOMO and LUMO energy levels of the polymers were calculated to be −5.27 eV, −5.01 eV, −4.94 eV and −3.57 eV, −3.66 eV, −3.76 eV, respectively. The electrochemical band gaps calculated from the HOMO-LUMO levels of polymers **PDTPTBT**, **PDTPTBTB** and **PDTPTBTBI** were 1.70 eV, 1.35 eV and 1.18 eV, respectively. The resulting electrochemical band gap values of **PDTPTBT**, **PDTPTBTB** and **PDTPTBTBI** are quite similar to the optical band values calculated from the onset of absorption. The conduction bands of the three polymers were located above the conduction band of the $PC_{60}BM$, which ensure the possibility of the efficient electron transfer from the polymer to $PC_{60}BM$. The HOMO and LUMO energy levels of **PDTPTBT**, **PDTPTBTB** and **PDTPTBTBI** were included in Table 1.

3.4. BHJ solar cell properties

Each of polymers **PDTPTBT**, **PDTPTBTB** and **PDTPTBTBI** were used as an electron donor material in PSC device fabrication. The PSC devices were fabricated with the structure of ITO/PEDOT:PSS/ **PDTPTBT** or **PDTPTBTB** or **PDTPTBTBI**:$PC_{60}BM$ (1:1, 1:2 or 1:3 wt/wt)/LiF/Al. The active layer of the PSCs was sandwitched between the hole injecting (PEDOT:PSS) and electron transporting (LiF) layers and covered with ITO anode and Al cathode. The current density-voltage (*J*–*V*) characteristics of the PSC devices were measured under the illumination of AM 1.5 G (100 mW/cm^2) solar simulator and their corresponding *J*–*V* curves are shown in Fig. 4 and their corresponding characteristic parameters such as V_{oc}, J_{sc}, *FF* and *PCE* are summarized in Table 2. In every case, the *PCE* of the device fabricated from polymer:$PC_{60}BM$ (1:3 wt/wt) as an active layer was higher than that of the device fabricated from polymer:$PC_{60}BM$ (1:1 wt/wt) or polymer:$PC_{60}BM$ (1:2 wt/wt) active layer under the identical condition. From the preliminary OPV studies, the maximum *PCE* of 2.04% was obtained with the device fabricated from **PDTPTBT**:$PC_{60}BM$ (1:3 wt/wt) with a V_{oc} of 0.55 V, a J_{sc} of 8.91 mA/cm^2, and a FF of 42.09%. On the other hand, the PSC devices fabricated from **PDTPTBTB**:$PC_{60}BM$ (1:3 wt/wt) and **PDTPTBTBI**:$PC_{60}BM$ (1:3 wt/wt) showed relatively decreased *PCE* of 1.01% (V_{oc} of 0.48 V, J_{sc} of 6.48 mA/cm^2 and FF of 32.73%) and 0.70% (V_{oc} of 0.44 V, J_{sc} of 5.62 mA/cm^2 and FF of 28.20%), respectively, compared to that of the device fabricated from **PDTPTBT**:$PC_{60}BM$ (1:3 wt/wt). The higher content of $PC_{60}BM$ is expected to be more favorable for the efficient light harvesting and electron–hole separation and, consequently, the improved photovoltaic parameters such as J_{sc}, V_{oc} and *FF* increase the overall photovoltaic performances. However, when the content of $PC_{60}BM$ was increased further to 1:4 wt/wt and 1:5 wt/wt in polymer:$PC_{60}BM$ blends, the photovoltaic performances (*PCE*) for all three polymers were found to decrease with relatively lower J_{sc} and *FF* values compared to those of the device prepared from 1:3 wt/wt polymer:$PC_{60}BM$ blends. The HOMO energy level of the polymers **PDTPTBT**, **PDTPTBTB** and **PDTPTBTBI** was found to be deeper in the order of **PDTPTBT** > **PDTPTBTB** > **PDTPTBTBI**, which is correlated well with the obtained V_{oc} of the PSC obtained in this study. In contrast, the J_{sc} of the PSC devices prepared from the synthesized polymers were expected to be in the order of **PDTPTBT** < **PDTPTBTB** < **PDTPTBTBI**, but the experimental results showed that the order is reversed as like **PDTPTBT** > **PDTPTBTB** > **PDTPTBTBI**. Though, the absorption band

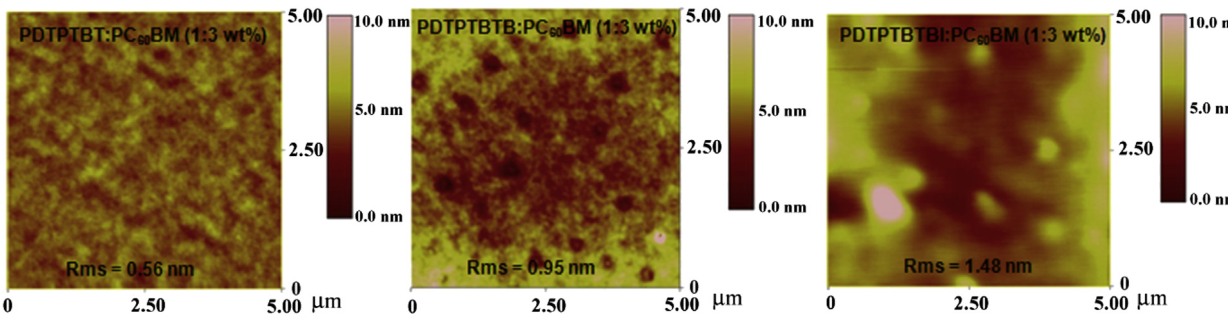

Fig. 5. AFM image obtained by tapping-mode on the surface for ITO/PEDOT:PSS/**PDTPTBT** or **PDTPTBTB** or **PDTPTBTBI**:$PC_{60}BM$ (1:3 wt/wt) subtracts.

of **PDTPTBTB** and **PDTPTBTBI** was found to be broader than that of **PDTPTBT**, relatively low molecular weight and lower band gap of the polymers are expected to decrease the carrier transport and charge dissociation at D–A interfaces [37,38]. Consequently, the photovoltaic parameters such as J_{sc} and *FF* were decreased for the devices prepared from the polymers **PDTPTBTB** and **PDTPTBTBI**. However, the overall *PCE* of **PDTPTBTB** and **PDTPTBTBI** was found to be quite better than previously reported near infrared (NIR) absorption polymers [23,36]. In addition, recently, NIR absorption polymers showing low band gap (1.30 eV) and energy levels similar to those of polymers **PDTPTBTB** and **PDTPTBTBI** were reported to give quite high PCE (around 9.5%) when they were used in triple layer solar cells along with relatively large band gap polymers even though they gave low *PCE* in single layer solar cells [39,40]. In this instance, polymers **PDTPTBTB** and **PDTPTBTBI** would be quite attractive for tandem solar cell applications.

The study on the surface of the active layer of PSCs is quite much important due to their strong influences on the photovoltaic performances [41]. The surface morphologies such as the donor-acceptor blending nature and smoothness of the active layers are usually studied by AFM analysis. In this instance, the surfaces of ITO/PEDOT:PSS/**PDTPTBT**, **PDTPTBTB** or **PDTPTBTBI**:$PC_{60}BM$ (1:3 wt/wt) substrates were subjected to AFM analysis and the AFM images of the active layers are shown in Fig. 5. The root-mean-square (rms) roughness of the active layers was determined to be 0.56, 0.95 and 1.40 nm, respectively and the blending between the polymer and $PC_{60}BM$ was found to better in the order of **PDTPTBT** > **PDTPTBTB** > **PDTPTBTBI**. From the AFM analysis, the overall energy conversion efficiency of the synthesized polymers **PDTPTBT**, **PDTPTBTB** and **PDTPTBTBI** is expected in the order of **PDTPTBT** > **PDTPTBTB** > **PDTPTBTBI**, and the *PCE* obtained in this study was found to be correlated well with the AFM results.

4. Conclusions

In this study, we prepared three new polymers such as **PDTPTBT**, **PDTPTBTB** and **PDTPTBTBI** and applied them to the fabrication of bulk heterojunction PSCs. The alternating polymer **PDTPTBT** was prepared by copolymerizing *N*-aryl DTP and TBT units. The optical and electrochemical studies of **PDTPTBT** indicated that the absorption band is extended from 300 nm to 750 nm and their HOMO and LUMO energy levels are located at -5.21 eV and -3.57 eV, respectively. As an effort to extend the absorption of **PDTPTBT**, we incorporated 2,1,3–benzothiadiazole or 2,2-dimethyl-2H-benzimidazole in polymer **PDTPTBT** main chain to afford polymers **PDTPTBTB** and **PDTPTBTBI**, respectively. The absorption band of **PDTPTBTB** and **PDTPTBTBI** was found to be extended up to 1000 nm and 1200 nm, respectively. The solution processed PSC devices prepared from each of the three polymers with the configuration of ITO/PEDOT:PSS/polymer:$PC_{60}BM$ (1:1 wt/wt and 1:2 wt/wt and 1:3 wt/wt)/LiF/Al showed maximum *PCE* of 2.04%, 1.01% and 0.70%, respectively, for 1:3 wt/wt donor-acceptor blend ratio. Even though the absorption ability of **PDTPTBTB** and **PDTPTBTBI** is better than that of **PDTPTBT**, their too low band gaps and relatively low molecular weights are expected to be the reason of their poor photovoltaic performances. We believe that the low band gap polymers **PDTPTBTB** and **PDTPTBTBI** can be promising candidates for tandem structured PSCs and polymer **PDTPTBT** is expected to show increased performance under the condition of optimized photovoltaic device structure.

Acknowledgments

This research was supported by the New & Renewable Energy program of the Korea Institute of Energy Technology Evaluation and Planning (KETEP) grant (No. 20103020010050) funded by the Ministry of Knowledge Economy, Republic of Korea.

References

[1] Park HJ, Kang M-G, Ahn SH, Guo LJ. Adv Mater 2010;22:E247–53.
[2] Søndergaard R, Hösel M, Angmo D, Larsen-Olsen TT, Krebs FC. Mater Today 2012;15:36–49.
[3] Chen H-Y, Hou J, Zhang S, Liang Y, Yang G, Yang Y, et al. Nat Photonics 2009;3:649–53.
[4] Liang Y, Xu Z, Xia J, Tsai S-T, Wu Y, Li G, et al. Adv Mater 2010;22:E135–8.
[5] Chu T-Y, Lu J, Beaupre S, Zhang Y, Pouliot J-R, Wakim S, et al. J Am Chem Soc 2011;133:4250–3.
[6] Son HJ, Wang W, Xu T, Liang Y, Wu Y, Li G, et al. J Am Chem Soc 2011;133:1885–94.
[7] Price SC, Stuart AC, Yang L, Zhou H, You W. J Am Chem Soc 2011;133:4625–31.
[8] Small CE, Chen S, Subbiah J, Amb CM, Tsang S-W, Lai T-H, et al. Nat Photonics 2012;6:115–20.
[9] Dou L, You J, Yang J, Chen C-C, He Y, Murase S, et al. Nat Photonics 2012;6:180–5.
[10] You J, Dou L, Yoshimura K, Kato T, Ohya K, Moriarty T, et al. Nat Commun 2013. http://dx.doi.org/10.1038/ncomms2411.
[11] Lunt RR, Osedach TP, Brown PR, Rowehl JA, Bulovic V. Adv Mater 2011;23:5712–27.
[12] Meng X, Zhang W, Tan Z, Li Y, Ma Y, Wang T, et al. Adv Funct Mater 2012;22:2187–93.
[13] Li W, Qin R, Zhou Y, Andersson M, Li F, Zhang C, et al. Polymer 2010;51:3031–8.
[14] Wang L, Fu Y, Zhu L, Cui G, Liang F, Guo L, et al. Polymer 2011;52:1748–54.
[15] Dong Y, Cai W, Hu X, Zhong C, Huang F, Cao Y. Polymer 2012;53:1465–72.
[16] Wang M, Li C, Lv A, Wang Z, Bo Z, Zhang F. Polymer 2012;53:324–32.
[17] Sun Y, Lin B, Yang H, Gong X. Polymer 2012;53:1535–42.
[18] Zeigler DF, Chen K-S, Yip H-L, Zhang Y, Jen AK-Y. J Polym Sci Part A: Polym Chem 2012;50:1362–73.
[19] Seo Y-H, Lee W-H, Park J-H, Bae C, Hong Y, Park J-W, et al. J Polym Sci Part A Polym Chem 2012;50:649–58.
[20] Jiang J-M, Yang P-A, Lan S-C, Yu C-M, Wei K-H. Polymer 2013;54:155–61.
[21] Tamilavan V, Song M, Jin S-H, Hyun MH. J Polym Sci Part A Polym Chem 2010;48:5514–21.
[22] Tamilavan V, Sakthivel P, Li Y, Song M, Kim C-H, Jin S-H, et al. J Polym Sci Part A: Polym Chem 2010;48:3169–77.
[23] Tamilavan V, Song M, Jin S-H, Hyun MH. Synth Met 2011;161:1199–206.
[24] Tamilavan V, Song M, Jin S-H, Hyun MH. Curr Appl Phys 2012;12:S124–30.
[25] Tamilavan V, Song M, Ban T-W, Jin S-H, Hyun MH. Polym Bull 2012;69:439–54.
[26] Tamilavan V, Song M, Jin S-H, Hyun MH. Polymer 2011;52:2384–90.
[27] Tamilavan V, Song M, Jin S-H, Hyun MH. Macromol Res 2013;21:406–13.
[28] Tamilavan V, Song M, Jin S-H, Hyun MH. Bull Korean Chem Soc 2012;33:3845–8.
[29] Duan C, Huang F, Cao Y. J Mater Chem 2012;22:10416–34.
[30] Vanormelingen W, den Bergh KV, Verbiest T, Koeckelberghs G. Macromolecules 2008;41:5582–9.
[31] Hati S, Patra GK, Naskar JP, Drew MGB, Datta D. New J Chem 2001;25:218–20.
[32] Duff EJ. J Chem Soc (A) 1968:434–7.
[33] Naef R, Balli H. Helv Chim Acta 1978;61:2958–73.
[34] Song S, Jin Y, Park SH, Cho S, Kim I, Lee K, et al. J Mater Chem 2010;20:6517–23.
[35] Zhu Z, Waller D, Gaudiana R, Morana M, Muhlbacher D, Scharber M, et al. Macromolecules 2007;40:1981–6.
[36] Tamilavan V, Song M, Jin S-H, Park HJ, Yoon UC, Hyun MH. Synth Met 2012;162:1184–9.
[37] Schilinsky P, Asawapirom U, Scherf U, Biele M, Brabec CJ. Chem Mater 2005;17:2175–80.
[38] Moet DJD, Lenes M, Kotlarskia JD, Veenstra SC, Sweelssen J, Koetse MM, et al. Org Elect 2009;10:1275–81.
[39] Bijleveld JC, Zoombelt AP, Mathijssen SGJ, Wienk MM, Turbiez M, de Leeuw DM, et al. J Am Chem Soc 2009;131:16616–7.
[40] Li W, Furlan A, Hendriks KH, Wienk MM, Janssen RAJ. J Am Chem Soc http://dx.doi.org/10.1021/ja401434x.
[41] Kastner C, Susarova DK, Jadhav R, Ulbricht C, Egbe DAM, Rathgeber S, et al. J Mater Chem 2012;22:15987–97.